Supporting Information

***Rec. Nat. Prod*. 15:5 (2021) 414-419**

Cyclic Polyketides with α-Glucosidase Inhibitory Activity from *Endiandra kingiana* Gamble and Molecular Docking Study

Mohamad Nurul Azmi[1,*], Nur Amirah Saad[1], Mohamad Hafizi Abu Bakar[2], Mohammad Tasyriq Che Omar[3], Ahmad Nazif Aziz[4], Habibah A. Wahab[5], Sadia Siddiq[6], M. Iqbal Choudhary[6], Marc Litaudon [7] and Khalijah Awang[8]

[1]School of Chemical Sciences, Universiti Sains Malaysia, 11800 Minden, Pulau Pinang, Malaysia
[2]Bioprocess Technology Division, School of Industrial Technology, Universiti Sains Malaysia
[3]School of Distance Education, Universiti Sains Malaysia, 11800 Minden, Pulau Pinang, Malaysia
[4]Faculty of Science and Marine Environment, Universiti Malaysia Terengganu, 21030, Kuala Nerus Terengganu, Malaysia
[5]School of Pharmaceutical Sciences, Universiti Sains Malaysia, 11800 Minden, Pulau Pinang, Malaysia
[6]H.E.J Research Institute of Chemistry, International Centre for Chemical and Biological Sciences, University of Karachi, Karachi, Pakistan
[7]Institut de Chimie des Substances Naturelles, CNRS-ICSN UPR2301, Univ. Paris-Sud 11, av. de la Terrasse, 91198 Gif-sur-Yvette, France
[8]Department of Chemistry, Faculty of Science, University of Malaya, 50603 Kuala Lumpur, Malaysia

	Table of Contents	Page

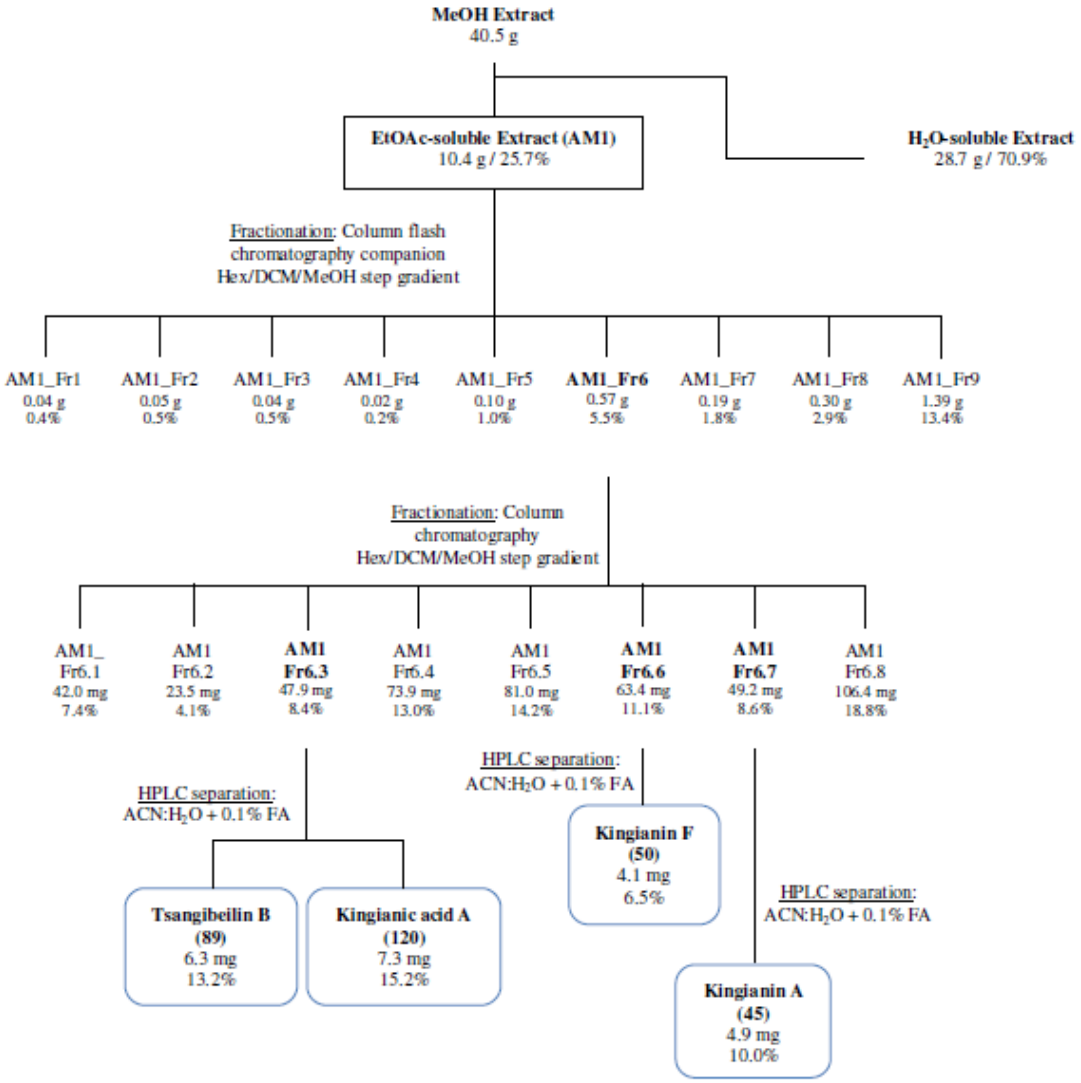

Figure S1: Separation and isolation scheme for compound **1** – **4**

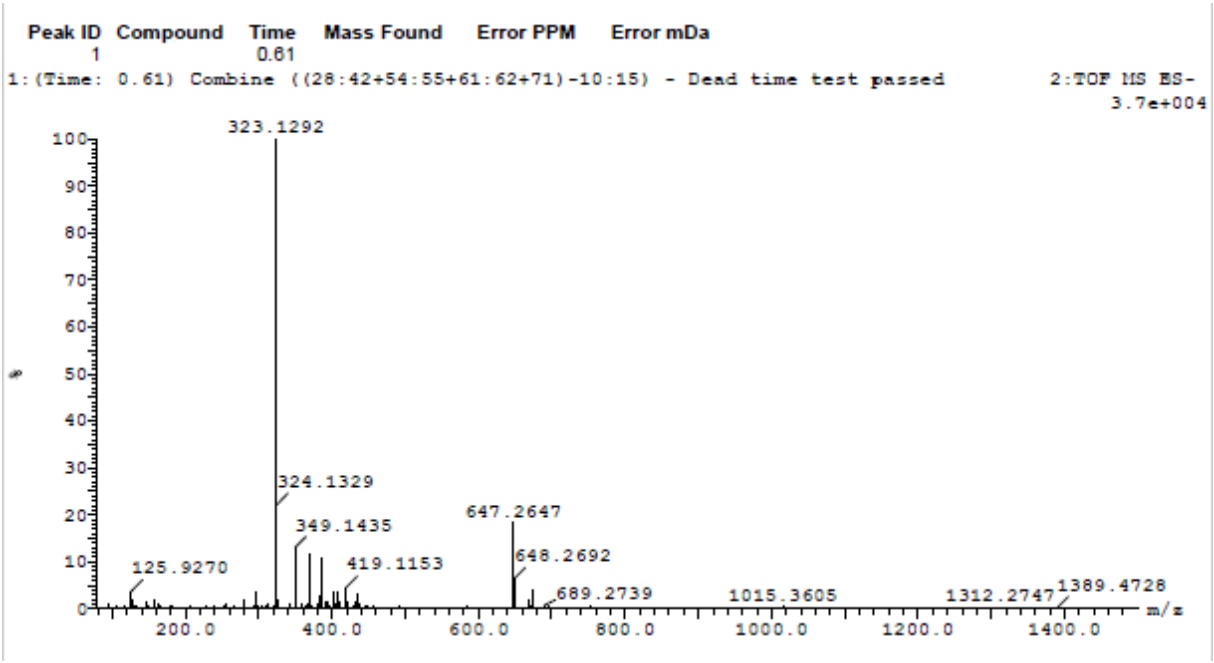

Figure S2: HRESIMS spectrum for compound **1**

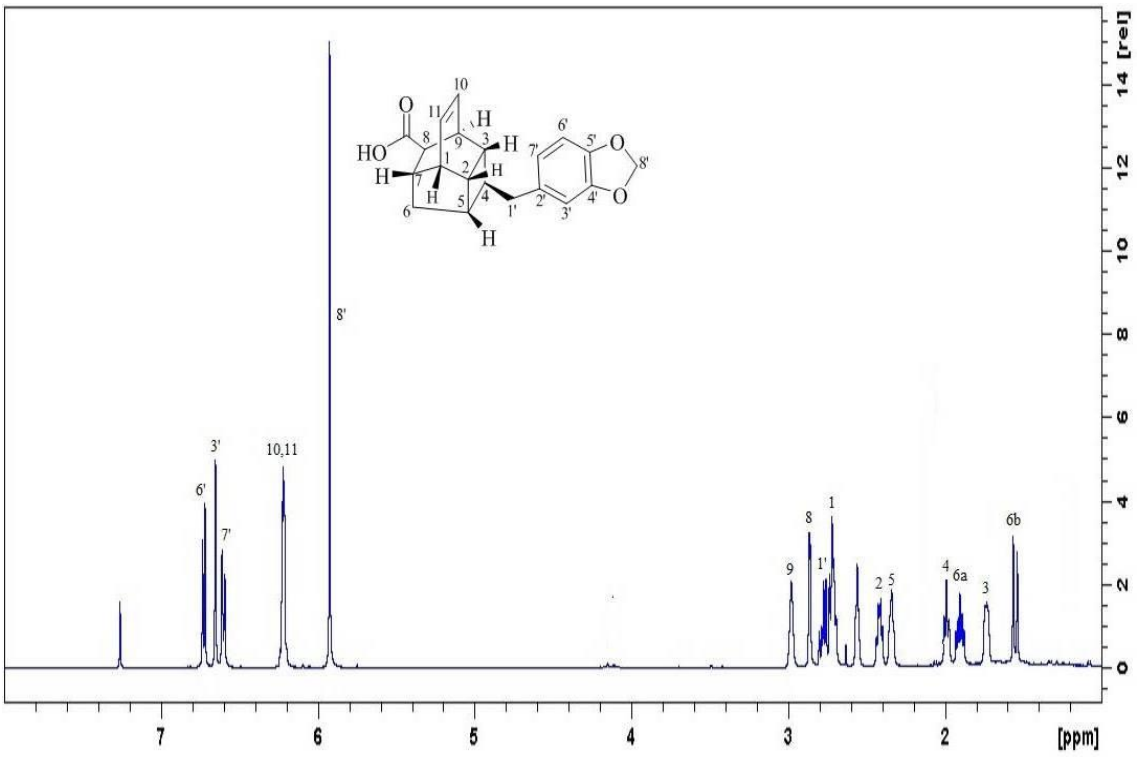

Figure S3: ^{1}H NMR spectrum for compound **1**

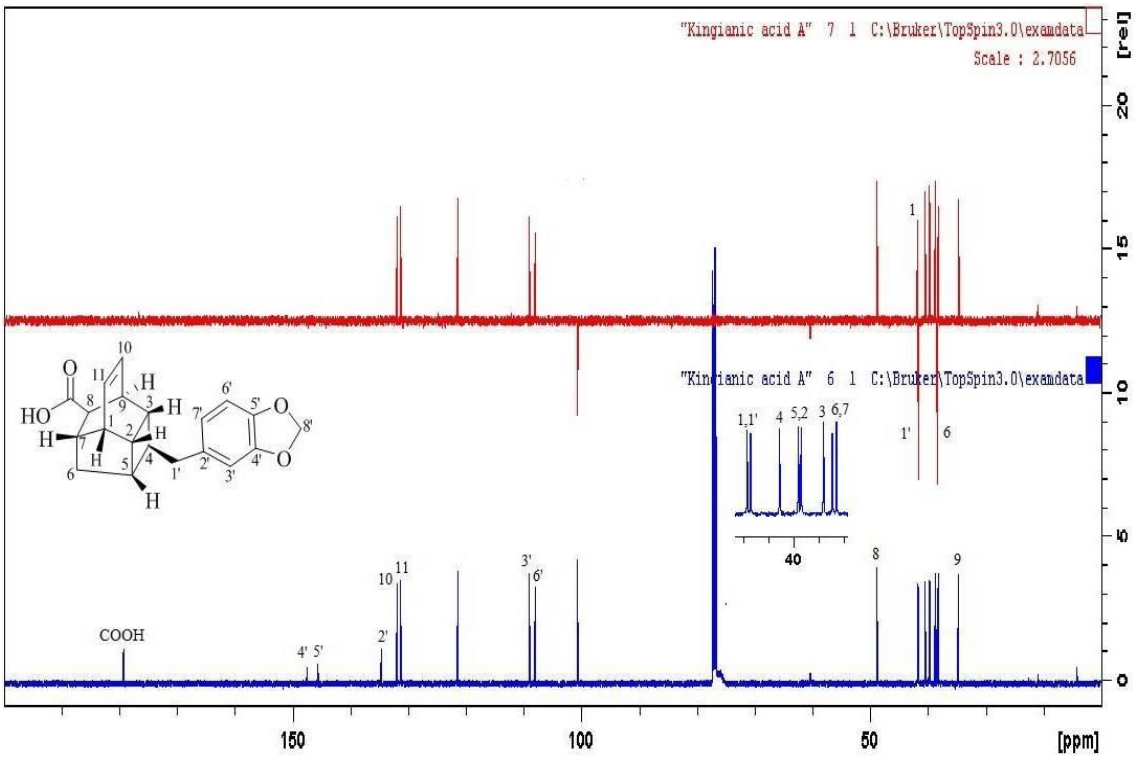

Figure S4: ^{13}C NMR and DEPT-135 spectrum for compound **1**

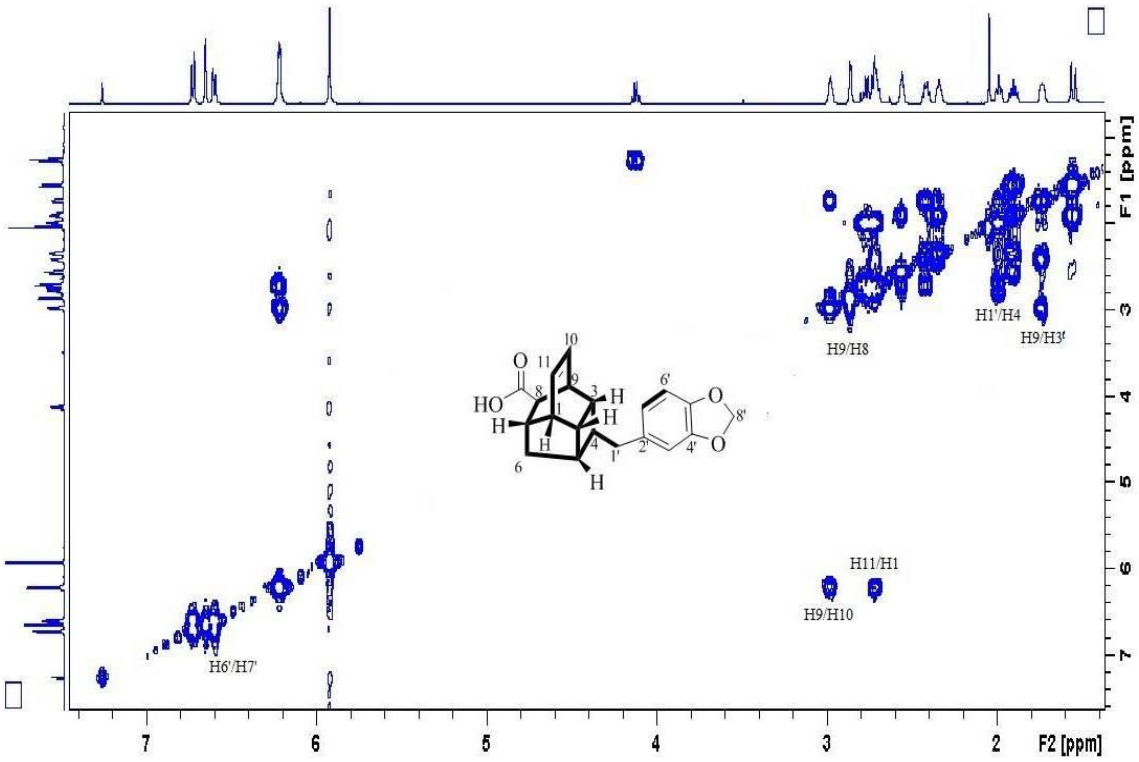

Figure S5: COSY-2D NMR spectrum for compound **1**

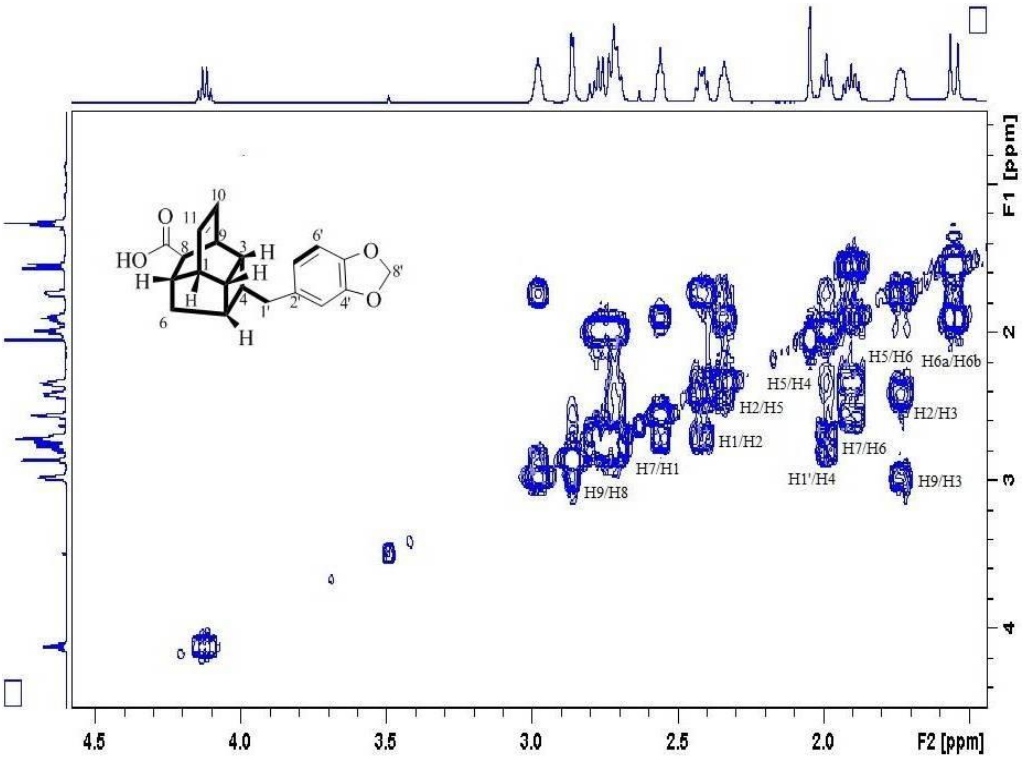

Figure S6: COSY-2D NMR (expanded) spectrum for compound **1**

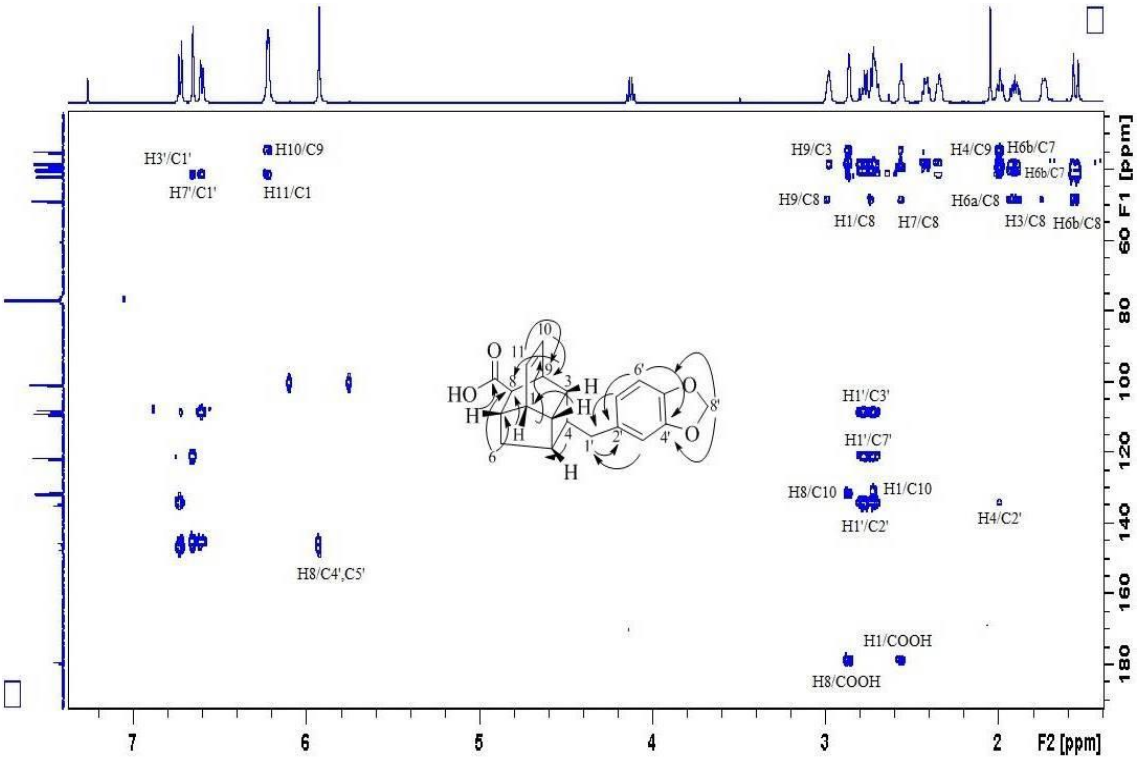

Figure S7: HMBC-2D NMR spectrum for compound **1**

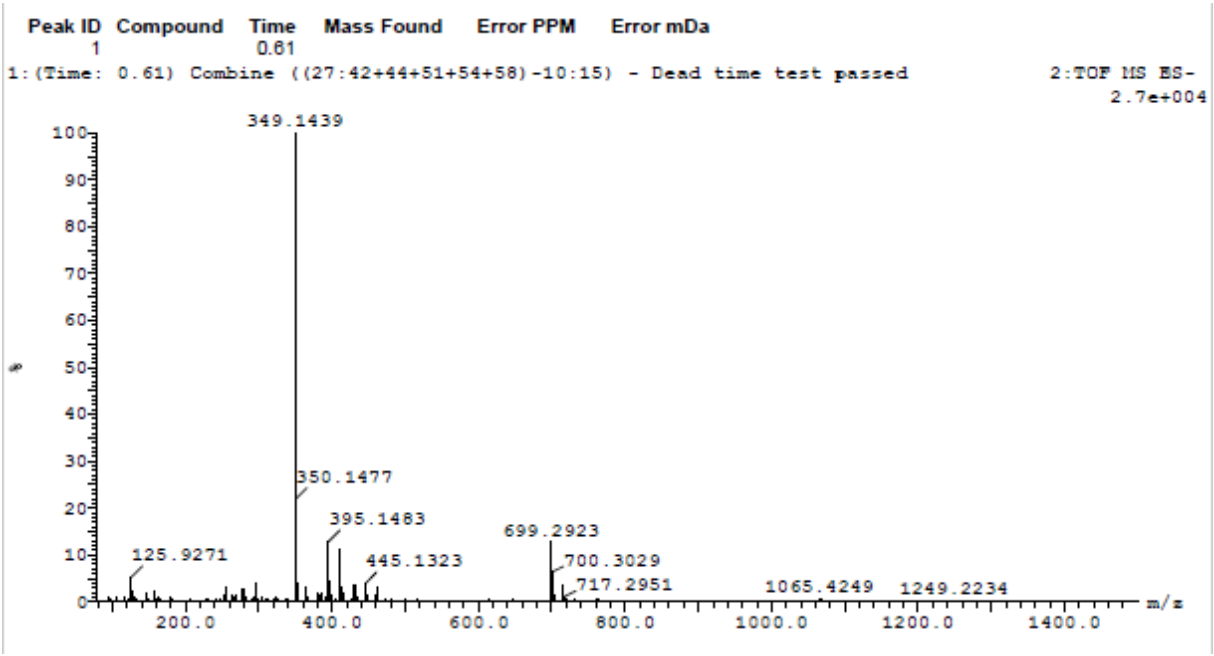

Figure S8: HRESIMS spectrum for compound **2**

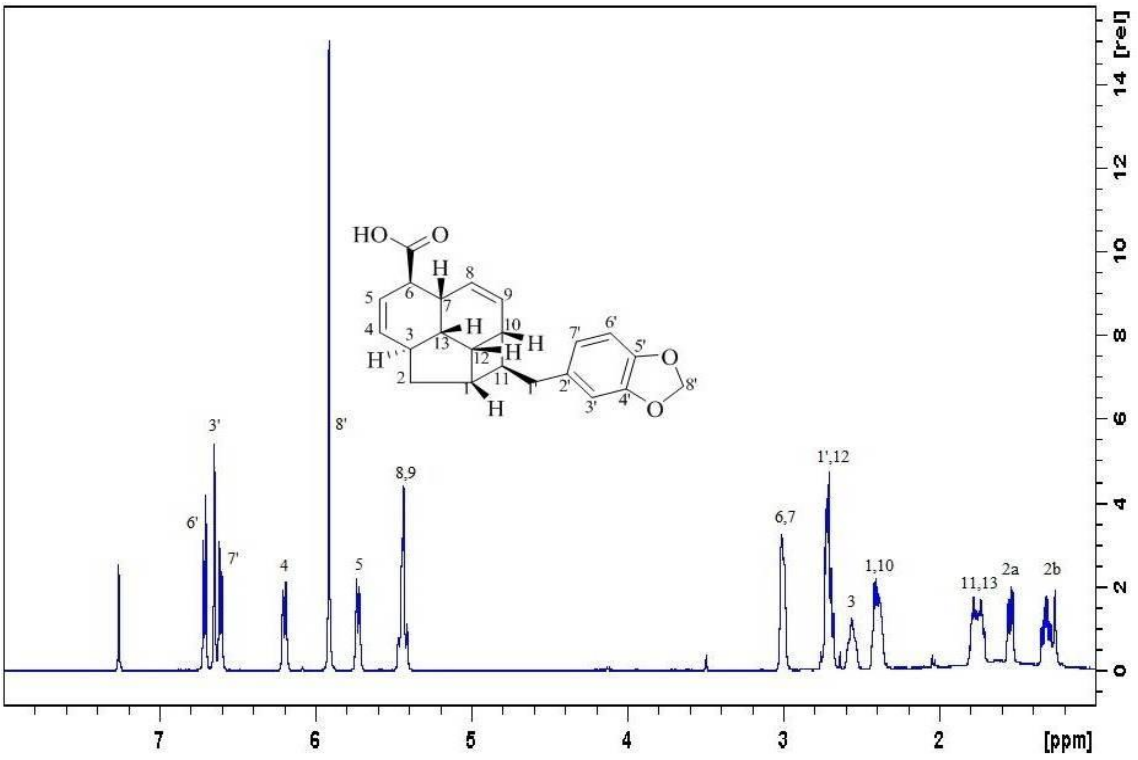

Figure S9: ^{1}H NMR spectrum for compound **2**

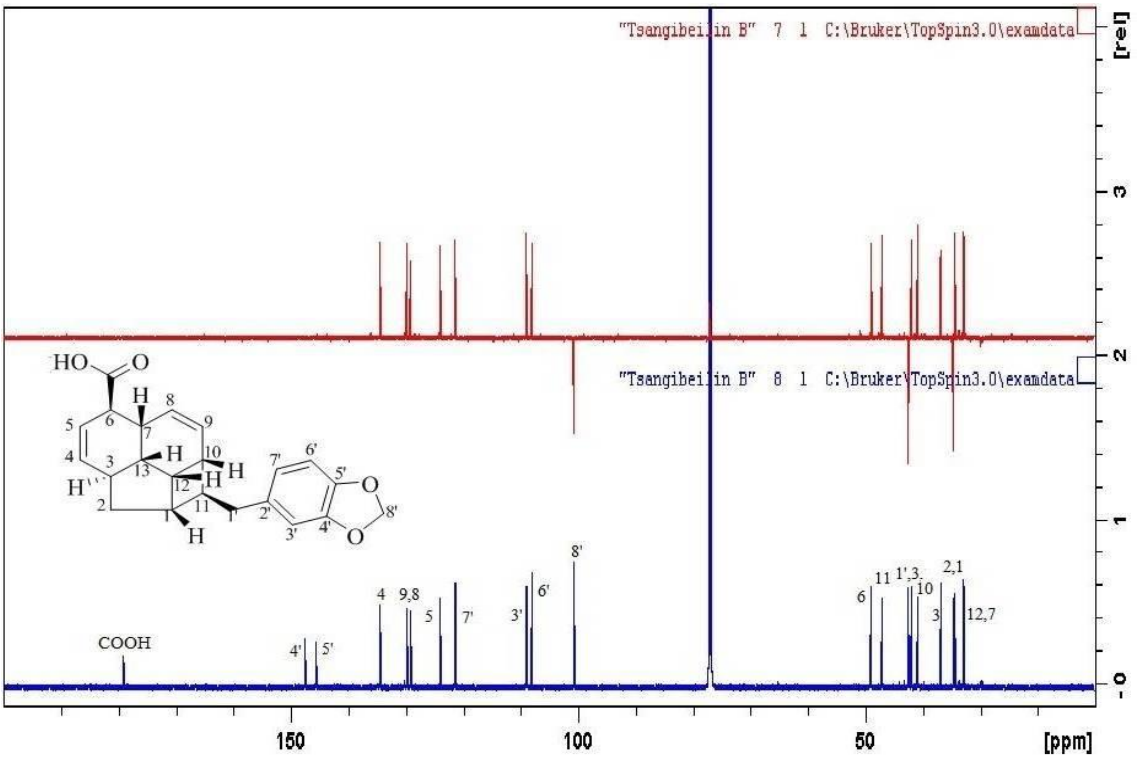

Figure S10: ^{13}C NMR and DEPT-135 spectrum for compound **2**

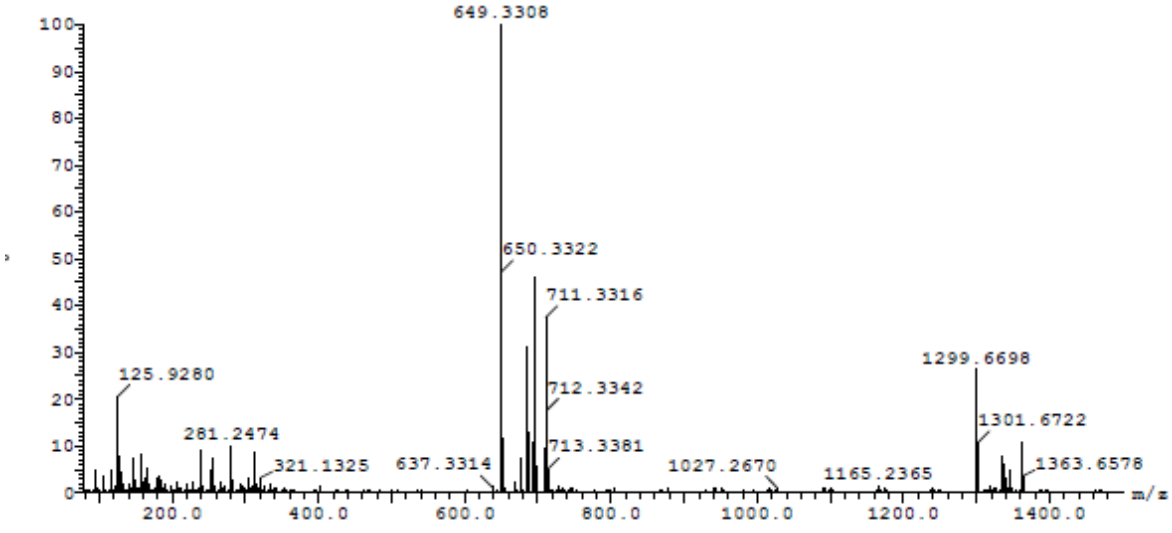

Figure S11: HRESIMS spectrum for compound **3**

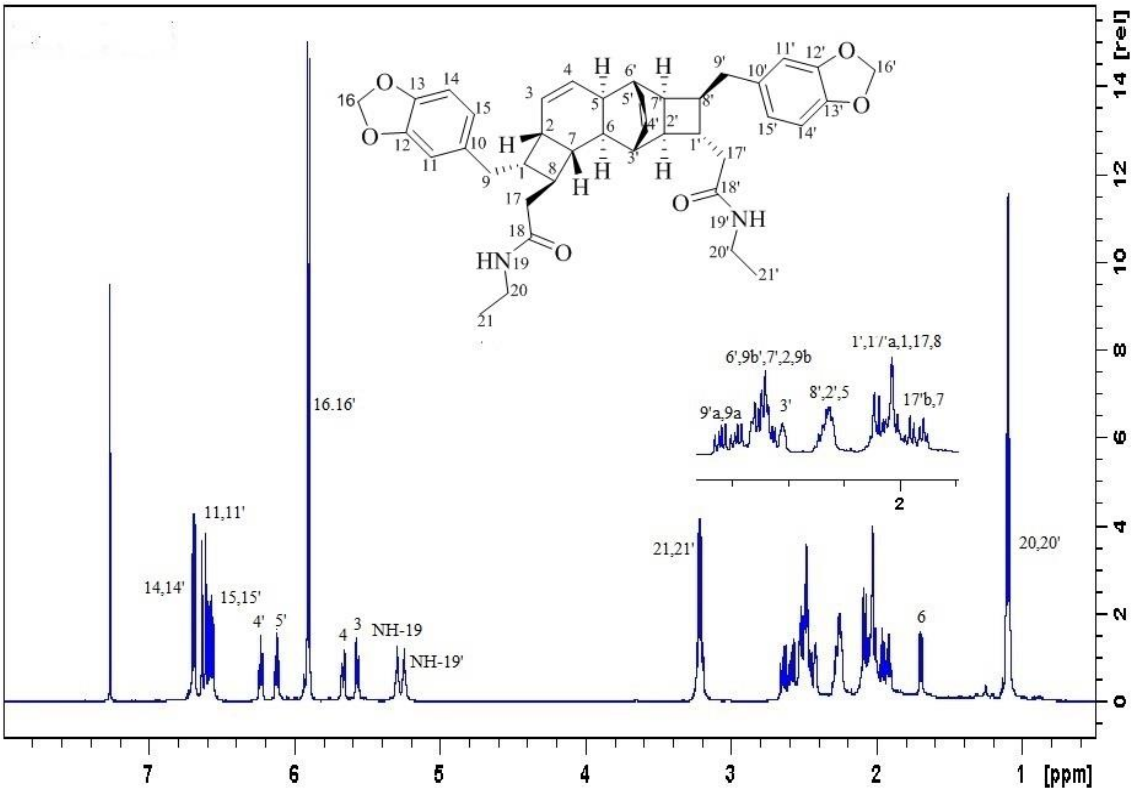

Figure S12: ^{1}H NMR spectrum for compound **3**

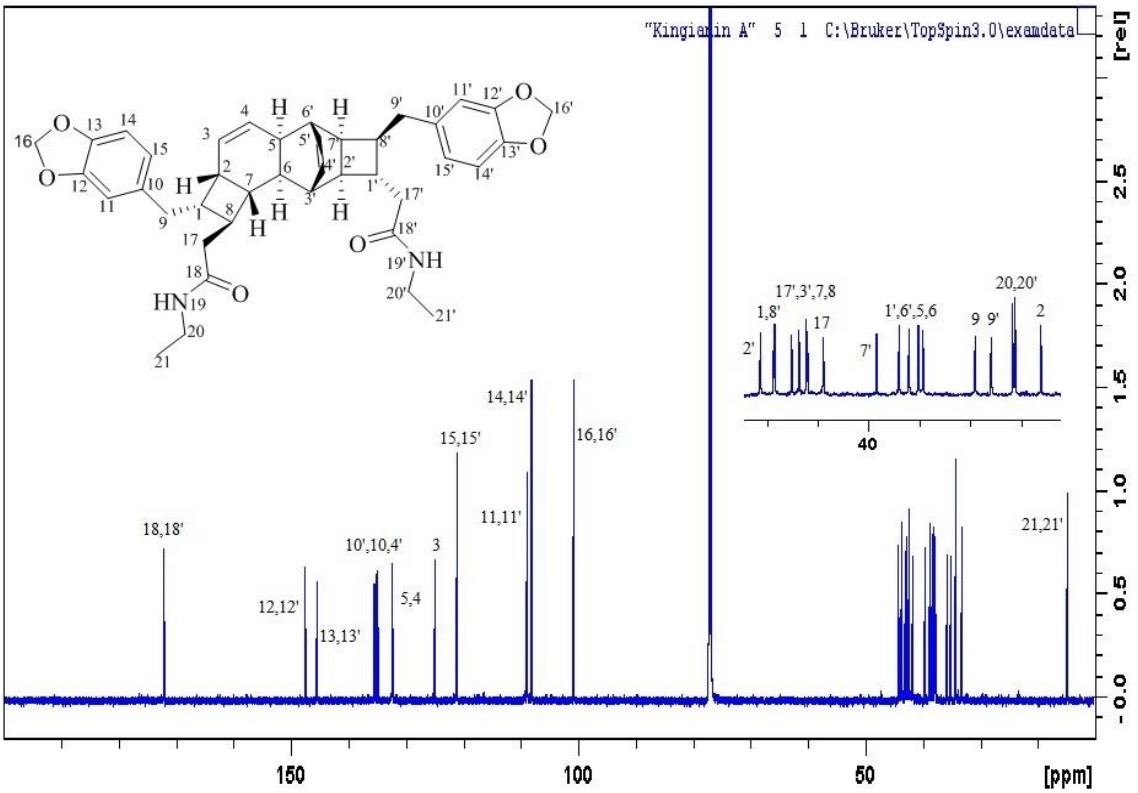

Figure S13: ^{13}C NMR spectrum for compound **3**

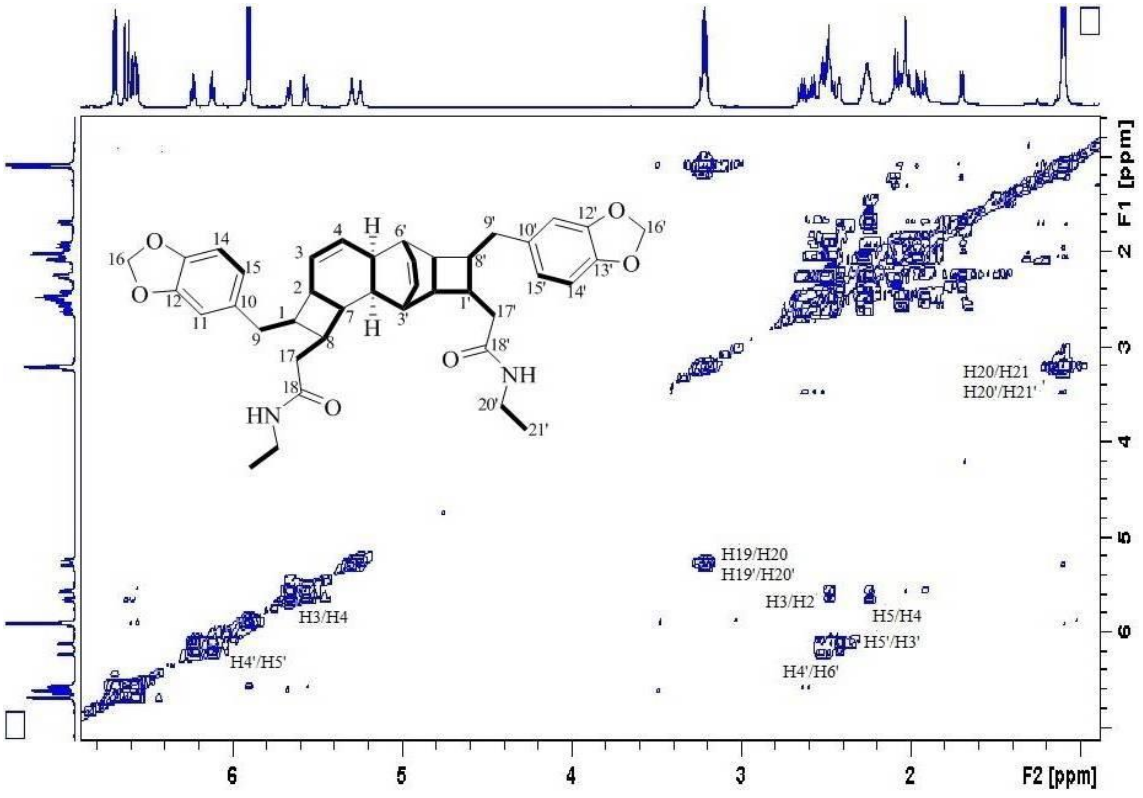

Figure S14: COSY-2D NMR spectrum for compound **3**

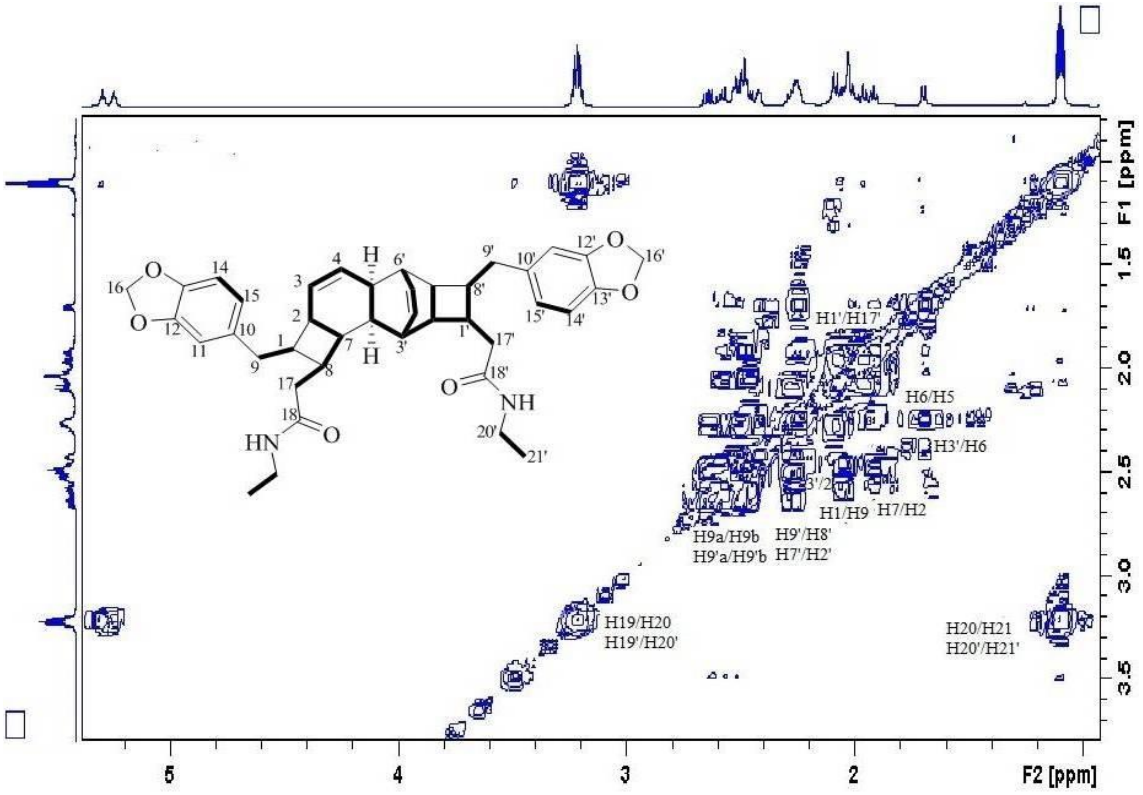

Figure S15: COSY-2D NMR (expended) spectrum for compound **3**

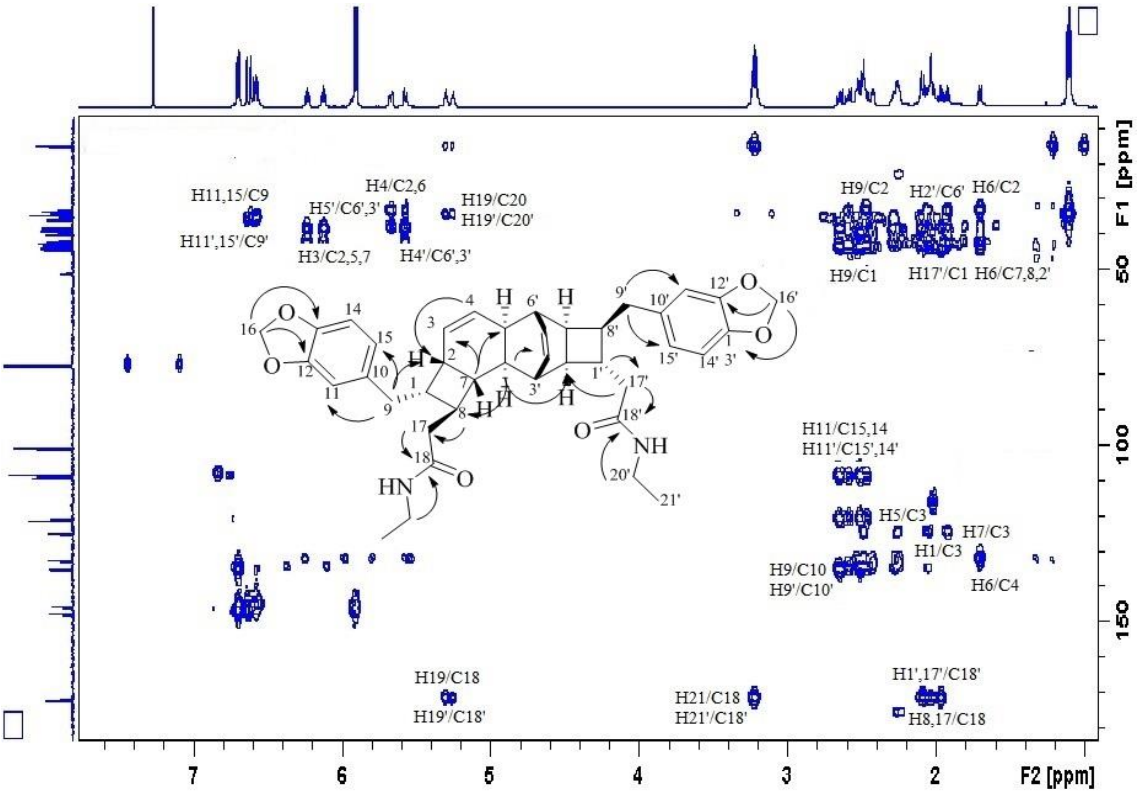

Figure S16: HMBC-2D NMR spectrum for compound **3**

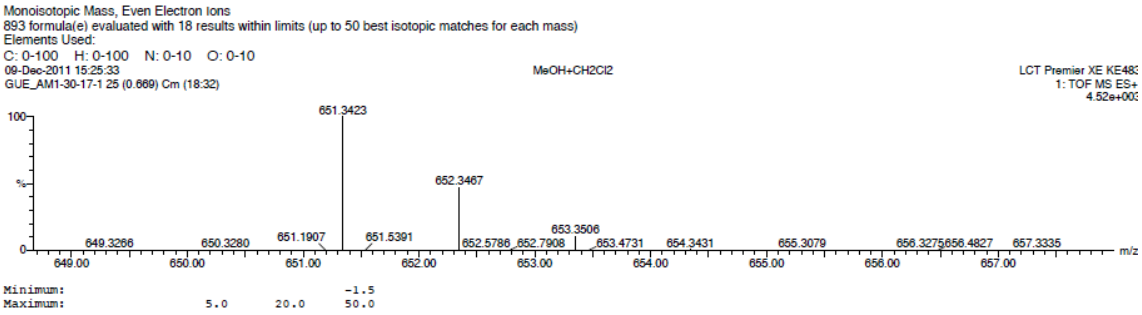

Figure S17: HRESIMS spectrum for compound **4**

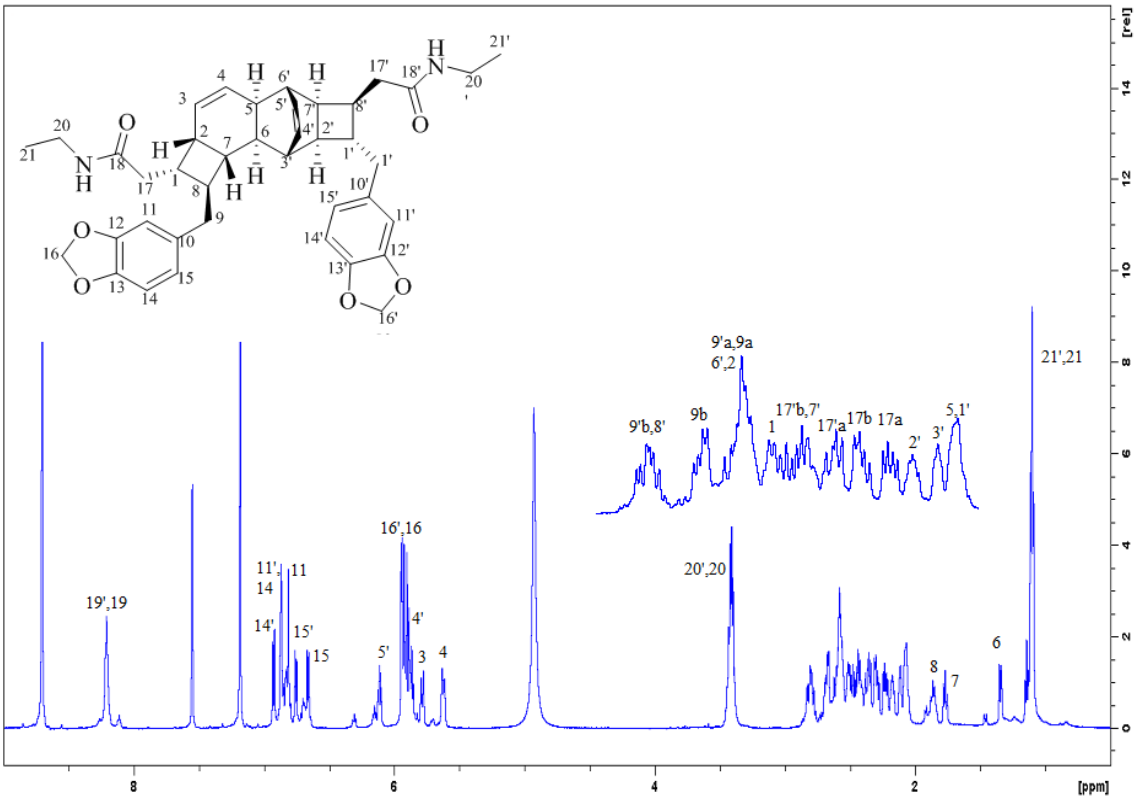

Figure S18: ^{1}H NMR spectrum for compound **4**

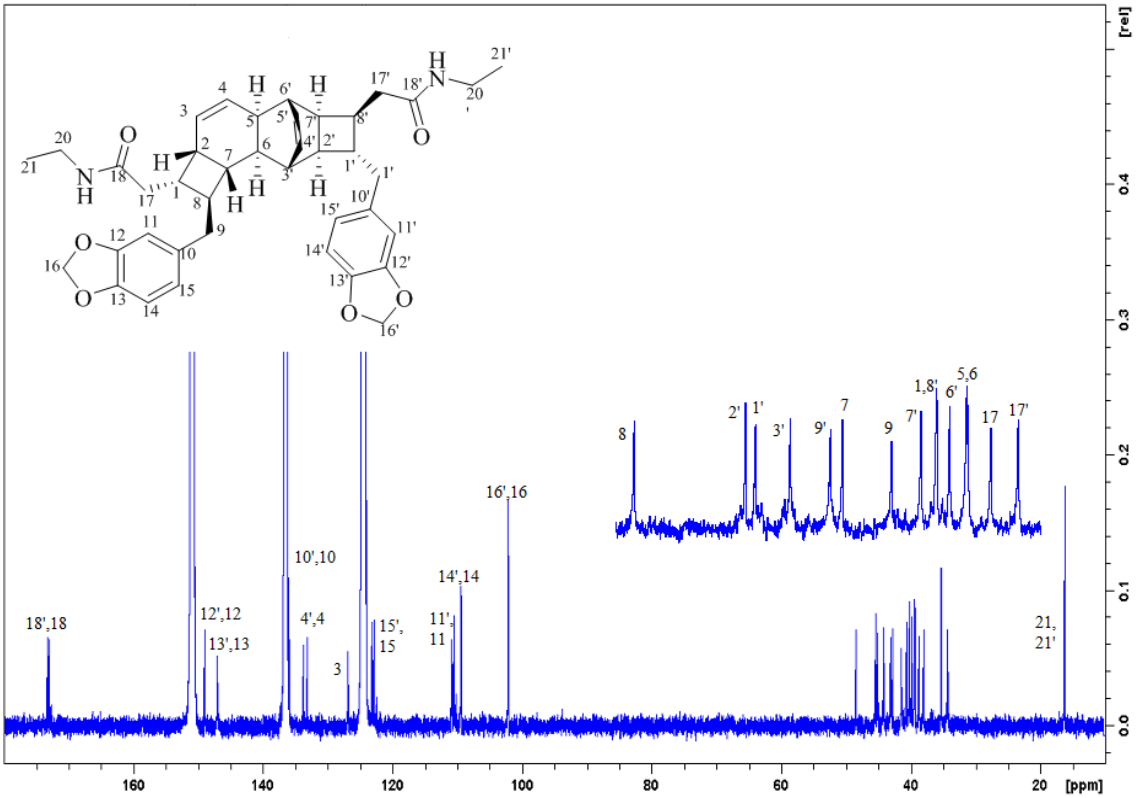

Figure S19: ^{13}C NMR spectrum for compound **4**

S1: *Preparation of stock solution:*
Briefly, the phosphate saline buffer was prepared with 50 mM with pH 6.8. Then, 4.214 mg of substrate solution (4-Nitrophenyl α-D-glucopyranoside) was prepared in 2500µl of phosphate buffer to the final concentration of 0.7 mM. Then, 0.022 mg of the enzyme (*α*-glucosidase from *Saccharomyces cerevisiae)* was dissolved in 2000 µl of the buffer which contains 0.04 u /well. To make 1 mM solution of inhibitor, 0.641 mg of Acarbose was dissolved in 75 µl of 70 % DMSO. In this experiment, 70% DMSO was used for control and to dissolve the test compounds

S2: *α-glucosidase enzyme inhibition activity*:
An *in vitro* antidiabetic activity for tsangibeilin B (**2**), kingianin A (**3**), and kingianin F (**4**) were measured using α-glucosidase inhibition assay on 96-well microtite plates using *α*-glucosidase from *Saccharomyces cerevisiae.* 135 µL of 50 mM phosphate saline buffer with pH 6.8 was dispended into the 96-well plates. Then, 20µL of the test sample in 70% DMSO and 20µl of the enzyme were added into the wells. The reaction mixture was incubated at 37.5 ℃ for 15 minutes. After the incubation period, a pre-read of the plate was taken by the spectra max. Next, 25µl of the substrate (pNPG) was added and the reading was taken on spectra max at 400 nm for 30 minutes. In the end normal read is taken and the percent inhibition was calculated.

$$\text{Percentage of inhibition (\%)} = \left(\frac{\text{Abs}_{\text{control}} - \text{Abs}_{\text{extract}}}{\text{Abs}_{\text{control}}}\right) \times 100$$

Table S1: Binding interactions details of compound **2-4** docked into N-terminal and C-terminal of human MGAM

Protein	Compounds	Free energy of binding	Protein Residue	Type of interaction
NtMGAM	2	-5.39	TYR299	π-π T-shaped
				π-alkyl
				π-sigma
			TRP441	π-alkyl
			TRP539	π-alkyl
			PHE575	π-alkyl
				π-π T-shaped
			HIS600	π-alkyl
			GLN603	H-bond
			TYR605	H-bond

	3	-7.50	THR205 ASN207 LEU473 PHE544 ALA576 TYR605	H-bond H-bond alkyl H-bond π-alkyl H-bond carbon π-π T-shaped
	4	-6.80	MET444 ASP542 ALA576 LEU577 TYR605	alkyl H-bond π-alkyl π-alkyl alkyl H-bond
	Acarbose	-3.23	ASN207 THR544 ALA545 THR546 TRP547 ASP548 ASP549	H-bond H-bond H-bond H-bond carbon H-bond carbon H-bond H-bond carbon H-bond Attractive charge Salt bridge Attractive charge
CtMGAM	2	-7.11	TRP1369 PHE1427 LYS1460 ASP1526 PHE1560	π-alkyl π-alkyl H-bond π-anion π-alkyl
	3	-10.87	PRO1159 LYS1164 ASP1420 LYS1460 PHE1560 THR1586	alkyl H-bond π-anion H-bond π-alkyl H-bond
	4	-10.48	TRP1355 TRP1369 ARG1377 MET1421 LYS1460	π-π stacked π-π T-shaped π-alkyl H-bond π-sulfur H-bond

		ASP1526	π-anion
		PHE1560	π-alkyl
		GLY1588	Unfavorable donor-donor
Acarbose	-10.17	ASP1157	H-bond
		GLN1158	H-bond
			H-bond carbon
		LYS1164	H-bond
		ASP1279	H-bond carbon
			H-bond
		ASP1420	Attractive charge
		GLU1451	H-bond
		LYS1460	H-bond
		ARG1510	H-bond
		ASP1526	Salt bridge
		HIS1584	H-bond

S3: *Molecular docking*:

The docking process using AutoDockTool 1.5.6 and Autodock 4.2 involved four steps: the preparation of reference structures (receptors and inhibitor), the preparation of ligands structures (compounds), docking and scoring, and visualization. The reference structures used were N-terminal of human Maltase-Glucoamylase (MGAM) complexed with acarbose (PDB ID: 2QMJ) and C-terminal of human Maltase-Glucoamylase (MGAM) complexed with acarbose (PDB ID: 3TOP), which downloaded from the RCSB PDB website. Briefly, both crystal PDBs were processed using UCSF Chimera software [12], starting by removing water molecules and unrelated heteroatom, followed by the separation of receptor and inhibitor from the complexes into individual structures and finally minimization of individual structures by steepest descent steps. Then, the minimized receptors and inhibitor were saved as PDB formats. The structures of all compounds were built using ChemDraw [13] and subsequently converted from cdx format to PDB.

Simulations of ligand-receptor docking were carried out using Autodock 4.2 software run with a Lamarckian genetic algorithm (LGA) search method [14-15]. AutoDockTools 1.5.6 was used for the generation of input files (rec.pdbqt and lig.pdbqt), the set-up of grid parameter file (rec.gpf) and the production of docking parameter file (lig.dpf). The active site of N-terminal and C-terminal of MGAM were enclosed in the center of the grid box having the size of -29.937, -6.184, -5.476 and -31.713, 35.676, 26.262 points in x, y, z direction respectively, which were the center points for the control (acarbose) binding sites in N-terminal and C-terminal of MGAM. Autogrid4 was executed to generate grid maps log file (rec.glg) for use with Autodock4. During docking, the receptors (N-terminal and C-terminal of MGAM) were set as rigid and the ligands (inhibitor and compounds) were set as flexible. The number of docking runs per simulation was 100 and the output of ligand poses, the docked coordinates, cluster sizes and free energy of binding were generated in the docking log file (lig.dlg). Visual inspection of poses and MGAM-ligands interactions were analyzed using Biovia Discovery Studio Visualizer Client 2020 (Dassault Systèmes BIOVIA, Discovery Studio Modeling Environment, Release 2017, San Diego: Dassault Systèmes, 2016).

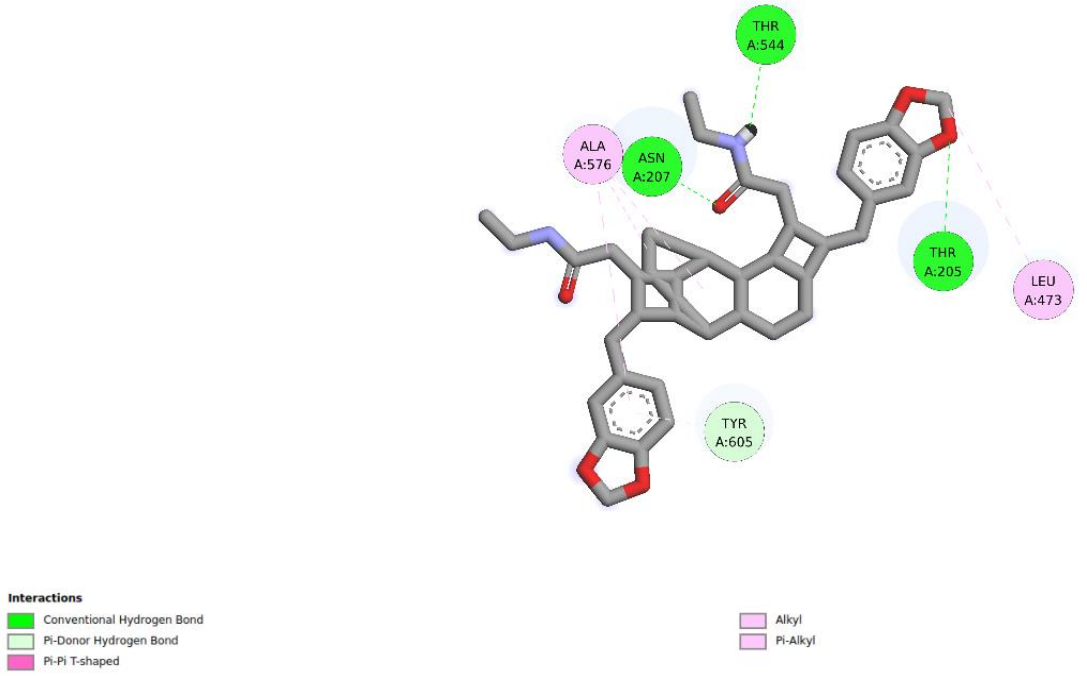

Figure S20: Two-dimensional binding modes of compound **3** present at active site of N-terminal of human MGAM

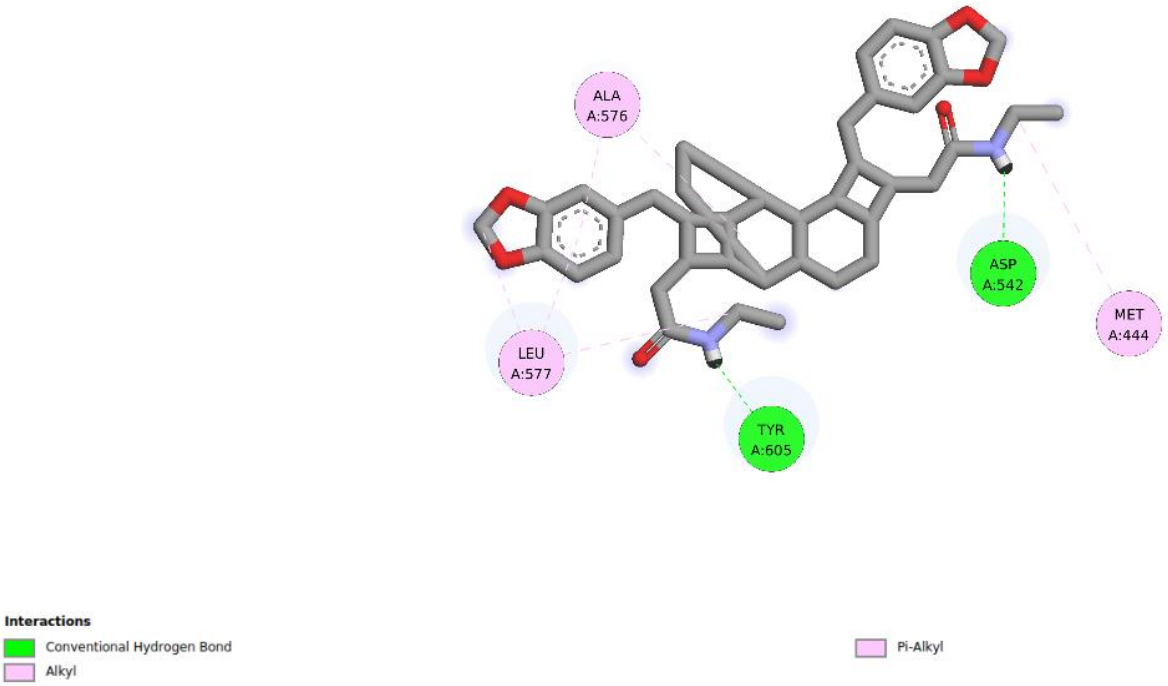

Figure S21: Two-dimensional of binding modes compound **4** present at active site of N-terminal of human MGAM